Open Access Library Journal

The Influence of the Carbon Surface on the Rate of Copper Recovery from Slag of the Direct-to-Blister Process

Piotr Madej, Marian Kucharski

Department of Metallurgy of Non-Ferrous Metals, AGH University of Science and Technology, Kraków, Poland
Email: markuch@neostrada.pl

Received 7 September 2014; revised 15 October 2014; accepted 17 November 2014

Abstract

The study was devoted to the investigation of the influence of the carbon reducer's surface on the rate of the copper removal (in the form of a copper-reach alloy, Cu-Pb-Fe) from the slag produced in the flash direct-to-blister process at the Głogów smelter in Poland. The slag used in this work was taken from the direct-to-blister Outokumpu flash furnace at the smelter in Głogów. Graphite penetrators of different surfaces were used as the slag reducer, and the experiments were carried out at 1573 K. It was found that the rate of the de-coppering process of the "Głogów" slag increased with the increase of the reducer's surface. The rate of the copper reduction from the slag in the form of Cu-Pb-Fe alloys was identified with the oxygen removal from this slag and described by the equation: $\frac{dn_{[O]}}{dt} = S \cdot k \cdot n_{[O]}^{n}$, where: $n_{[O]}$—the number of the oxygen moles which could be removed from the slag; S—the surface on which the reduction took place (it was assumed that it is equal to the penetrator area); k—the rate constant; n—the exponent. It was found that the reaction rate "constant" as well as the exponent n increased with the increase of the superficial gas velocity, which was caused by the decrease in the gaps between the crucibles and the graphite penetrators. Therefore, it can be concluded that the reduction process was very likely controlled by the convective mass transfer.

Keywords

Outokumpu Direct-to-Blister Process, Slag, Kinetics

Subject Areas: **Material Experiment, Metal Material**

How to cite this paper: Madej, P. and Kucharski, M. (2014) The Influence of the Carbon Surface on the Rate of Copper Recovery from Slag of the Direct-to-Blister Process. *Open Access Library Journal*, **1**: e1057.
http://dx.doi.org/10.4236/oalib.1101057

1. Introduction

In the recent years, an increasing attention has been paid to the reaction of a metal oxide in the liquid state with solid carbon. Numerous studies [1]-[11] have been carried out on the kinetics of the reduction of iron oxide from liquid slag by solid carbon or carbon dissolved in liquid iron. There have been large discrepancies among the results of different researchers regarding the magnitude of the constant rate and the controlling steps of the overall process. The reduction process is undoubtedly a complex one and is characterized by a gas film which forms quickly around the solid carbon particles. In the steady state, the reduction proceeds with gaseous intermediates between the carbon and the slag, and the overall process is a combination of sequential reactions at different interfaces:

1) the mass transfer of the reducible metal oxide to the gas/slag interface from the slag bulk,
2) the chemical reaction of CO with the metal oxide at the gas/slag interface,
3) the diffusion of the formed CO_2 towards the gas/carbon interface,
4) the chemical reaction of CO_2 with carbon to reproduce CO.

A number of studies [3] [6] [7] [11] have pointed to the fact that the mass transfer in the slag phase may be the limiting step of the reduction rate. However, several authors [1] [2] [4] [8] [9] have concluded that the Boudouard reaction is the rate controlling step. This view is based on the observation that the CO/CO_2 ratio of the generated gases is close to that which can be predicted by a thermodynamic calculation of the iron oxide reduction. However, the final result depends on the iron oxide activity in the slag.

Many other researchers [12]-[19] have studied the rates of the reduction/oxidation slags using CO + CO_2 mixtures, and again, there have been discrepancies among their results. Inconsistencies have been observed among the results of the studies of the values of the reaction rate, the mechanism of the reactions involved and the controlling steps.

There are very few experimental results in the literature for the molten copper bearing slag reduction. In the modern copper-making processes, e.g. direct-to-blister, the produced slags are reduced in an electric slag cleaning furnace. For this reason, in the present study, the rate of the overall reduction of the slag from the direct-to-blister process employed at the copper plant “Głogów” was investigated. In order to obtain a high productivity of the copper recovery from the slags, the reactive area between the slags and the carbon reducer should be as high as possible. In consequence, the effect of the reducer’s surface on the rate of the industrial slag reduction was investigated in this study. The attempt in early investigation on copper recovery from the slag of direct-to-blister process [20] to establish a relation between reduction rate and the reducer surface has failed, because of foaming of the investigated slag. However, not all the slags exhibited the tendency for foaming, and it so happened that the next slag portion from the copper plant “Głogów” did not foam.

2. Experimental Procedure

The aim of these investigations was to determine the influence magnitude of the reducer/slag interface on the kinetics of the slag reduction. Graphite penetrators were used as the slag reducer agent. A graphite penetrator was fixed onto an alumina tube, which made it possible for the penetrator to be immersed in the reduced slag. In this study, penetrators of different surfaces were used, and their shape can be seen in **Figure 1**.

In this study, four penetrators of different surfaces were employed. The dimensions of these penetrators and their surfaces are enclosed in **Table 1**.

3. Apparatus

The experimental arrangement and procedure were identical to those described earlier [20].

A schematic diagram of the apparatus used in this study is shown in **Figure 2**.

The slag reduction experiments were carried out in alumina crucibles placed in an alumina reaction tube and heated in a vertical laboratory electric furnace. The furnace temperature was maintained at ±2 K and the maximum temperature variation in the hot zone was ±3 K. The alumina reaction tube (70-mm i.d.) was sealed at the top and the bottom by means of water cooled brass caps and with the use of rubber O-rings. The measuring thermocouple Pt-PtRh10 was located close to the crucible with the investigated slag. The graphite penetrators were placed under the upper cap of the reaction tube. The experiment started when the graphite penetrator was

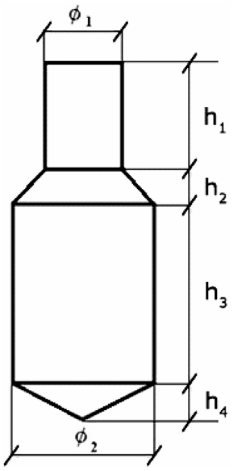

Figure 1. Shape of the graphite penetrators used in this study.

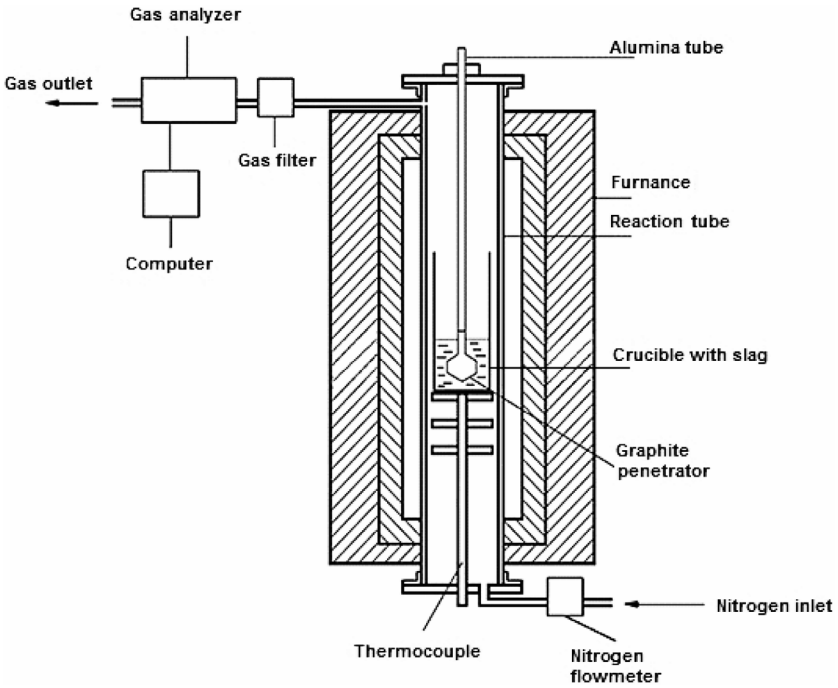

Figure 2. Schematic diagram of the experimental apparatus.

Table 1. Dimensions of the penetrators and their surfaces.

	Penetrator 1	Penetrator 2	Penetrator 3	Penetrator 4
ϕ_1, [mm]	11	11	11	11
ϕ_2, [mm]	15	20	25	30
h_1, [mm]	15	15	15	15
h_2, [mm]	5	5	5	5
h_3, [mm]	25	25	25	25
h_4, [mm]	5	5	5	5
S, [cm^2]	16.1	22.5	29.8	37.9

lowered to the controlled depth in the slag, followed by the temperature stabilization of the molten slag. Slag produced by the Głogów direct-to-blister flash smelter was used in this study. The main constituents of this slag are listed in **Table 2**.

An alumina crucible (i.d. = 45 mm, H = 77 mm + 200 mm extension) with 160 g of slag was placed in the reaction tube of the furnace. In the upper cap of the reaction tube, a graphite penetrator fixed to an alumina tube was situated. A high purity nitrogen stream of 25 Ndm^3/h flow rate was introduced into the reaction tube of the furnace through its bottom cap. After about 5 hrs, the furnace was switched on and the temperature controller was adjusted to 573 K. The furnace was kept under these conditions for approximately 12 hours. Next, the temperature of the furnace was increased to 1573 K. The sample was kept at this temperature for one hour with the purpose to stabilize the temperature of the slag. After the temperature of the slag stabilized, the graphite penetrator was immersed into the slag. The moment of the immersion of the graphite penetrator in the slag was taken as the beginning of the reduction process. However, the first signal of the reduction process was detectable after about 50 - 60 seconds from that moment. During the experiment, a gas composed of nitrogen, carbon monoxide and carbon dioxide was formed as a result of the reactions between the graphite and the slag. The CO and CO_2 were analyzed by a gas analyzer for CO and CO_2 every 5 seconds, and the results were recorded by the computer. Examples of a typical variation of the CO and CO_2 concentration in the N_2-CO-CO_2 gas mixture are given in **Figure 3** and **Figure 4**.

As can be seen from **Figure 3** and **Figure 4**, the results of these three series of independent experiments agree very well with each other.

4. Calibrations of the Gas Analyzer and Experimental Setup

The flow rates (in Ndm^3/h) of the CO and CO_2 formed during the reduction process were calculated from the relations:

$$V_{CO}^{i} = \frac{26.11 \cdot (\text{vol.} - \%CO)}{100 - 1.041 \cdot (\text{vol.} - \%CO) - 0.956 \cdot (\text{vol.} - \%CO_2)} \tag{1}$$

$$V_{CO_2}^{i} = \frac{23.98 \cdot (\text{vol.} - \%CO_2)}{100 - 1.041 \cdot (\text{vol.} - \%CO) - 0.956 \cdot (\text{vol.} - \%CO_2)} \tag{2}$$

These relations were established from the gas analyzer calibration procedure, which has been described in details elsewhere [20] [21]. When the penetrator is immersed in the investigated slag, reduction reactions take place, which generate CO and CO_2. However, the first gas analyzer readings were detected after about 50 - 60 seconds from the moment of the graphite penetrator's immersion. A part of these gases was cumulated in the reaction tube, and this fraction should also be taken into account. In order to estimate the real volumes of these gases, a calibration of the reaction tube was carried out [20]. According to this calibration, the volume of the cumulated CO and CO_2 can be expressed by the relations:

$$\Delta V_{CO}^{i} \ \left(Ndm^3\right) = 0.0219 \cdot V_{CO}^{i} \ \left(Ndm^3/h\right) \tag{3}$$

$$\Delta V_{CO_2}^{i} \ \left(Ndm^3\right) = 0.0219 \cdot V_{CO_2}^{i} \ \left(Ndm^3/h\right) \tag{4}$$

where: ΔV_{CO}^{i}, $\Delta V_{CO_2}^{i}$ —the volumes of the CO and CO_2, respectively, cumulated in the reaction tube, V_{CO}^{i}, $V_{CO_2}^{i}$ —the flow rates of the CO and CO_2, respectively, calculated with Equation (1) and Equation (2), $i = 1, 2, 3, 4, \cdots$, etc.—the number of the experimental points.

Therefore, the real flow rates of the CO and CO_2 passing through the reaction tube after $t = 5 \cdot i$ seconds can be obtained from the relations:

$$V_{CO(A)}^{i} = V_{CO}^{i} + \left(\Delta V_{CO}^{i} - \Delta V_{CO}^{i-1}\right) \cdot \frac{3600}{5} \tag{5}$$

$$V_{CO_2(A)}^{i} = V_{CO_2}^{i} + \left(\Delta V_{CO_2}^{i} - \Delta V_{CO_2}^{i-1}\right) \cdot \frac{3600}{5} \tag{6}$$

The second terms of Equations (5) and (6) have to be multiplied by the 3600/5 value, in order for the second

Table 2. Main components of the Głogów direct-to blister flush smelter slag used in this work.

Components	SiO_2	CaO	MgO	Al_2O_3	Na_2O	K_2O	Cu	Pb	Fe	Zn	As
% -wt.	33.94	15.60	4.94	10.00	0.75	2.39	12.45	3.05	8.06	1.13	0.192

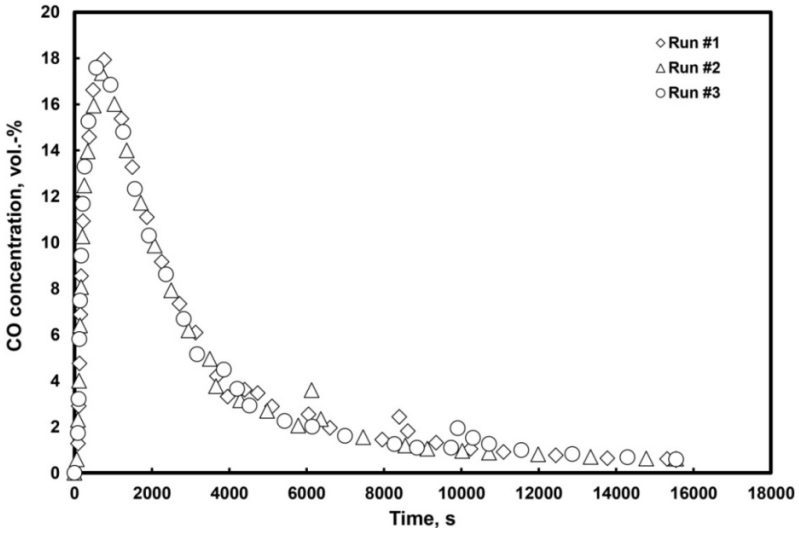

Figure 3. Typical changes of the CO concentrations in the gas leaving the reaction tube during the slag reduction with a graphite penetrator at 1573 K. For the sake of graph clarity, only about 1/10 of the experimental points are shown (all the experimental data in the Excel format are available on request).

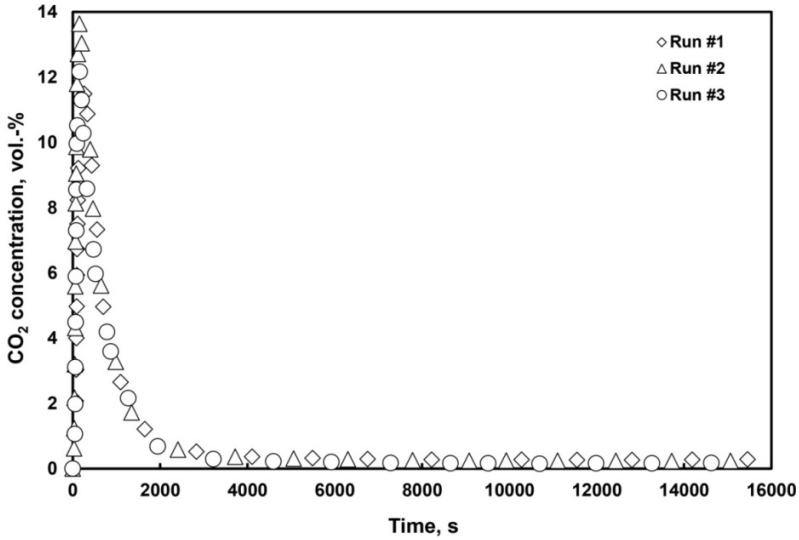

Figure 4. Typical changes of the CO_2 concentrations in the gas leaving the reaction tube during the slag reduction with a graphite penetrator at 1573 K. For the sake of graph clarity, only about 1/10 of the experimental points are shown (all the experimental data in the Excel format are available on request).

terms to be converted to the appropriate unit. As the analyzer readings were adjusted to 273 K (STP), the numbers of the CO and CO_2 moles per one second could be calculated from the relations:

$$n_{CO} = \frac{V^{i}_{CO(A)}}{22.4 \cdot 3600} \tag{7}$$

$$n_{CO_2} = \frac{V^i_{CO_2(A)}}{22.4 \cdot 3600} \tag{8}$$

The number of the oxygen moles reduced from the slag during a period of 5 seconds (5 seconds was the time between two consecutive measurements) was determined from the relation:

$$n_{[O]} = \frac{n^i_{CO} + n^{i+1}_{CO}}{2} \cdot 5 + 2 \cdot \frac{n^i_{CO_2} + n^{i+1}_{CO_2}}{2} \cdot 5 \tag{9}$$

where: n^i_{CO}, n^{i+1}_{CO}—the number of the CO moles formed during the reduction process per one second, recorded in two consecutive measurements, $n^{(i)}_{CO_2}$, $n^{i+1}_{CO_2}$—the number of the CO_2 moles formed during the reduction process per one second, recorded in two consecutive measurements.

The masses of the consumed carbon estimated from Equation (7) and Equation (8) were slightly lower than the loss of the masses of the graphite penetrators used in the experimental runs. The differences were of the order of 0.4% to 4%.

5. Results

By the summation of the $n_{[O]}$ values, calculated with Equation (9), the number of the oxygen moles removed from the slag as a function of the reduction time was determined. An example of these computations is presented in **Figure 5**.

The instantaneous rate of the process reduction may be determined directly with the use of the experimental data:

$$\frac{dn_{[O]}}{dt} \approx \frac{\Delta n_{[O]}}{\Delta t} = \frac{n^i_{[O]} - n^{i-1}_{[O]}}{5} \tag{10}$$

where: $n^{i+1}_{[O]}$, $n^i_{[O]}$—the numbers of the oxygen moles removed from the slag after $5 \cdot i$ and $5 \cdot (i+1)$ seconds of the reduction time, $i = 1, 2, 3, \cdots$, etc.—the numbers of the experimental points.

An example of the calculated values of $dn_{[O]}/dt$, in the case of the graphite penetrators with the surface area of 22.5 cm^2, is shown in **Figure 6**.

The dependence of the rate of the oxygen removal from the slag can be expressed by the equation:

$$\frac{d\left(n^0_{[O]} - n_{[O]}(t)\right)}{dt} = S \cdot k \cdot \left(n^0_{[O]} - n_{[O]}(t)\right)^n \tag{11}$$

where: $n^0_{[O]}$—the number of the oxygen moles which could be removed from slag, $n_{[O]}(t)$—the number of the oxygen moles removed from the slag within the time "t", S—the surface on which the reduction took place (it was assumed that it is equal to the penetrator area), k—the apparent rate constant, n—the exponent.

To estimate the k and n values, Equation (11) has to be expressed in the logarithmic form:

$$\ln\left(\frac{d\left(n^0_{[O]} - n_{[O]}(t)\right)}{dt}\right) = \ln(S \cdot k) + n \cdot \ln\left(n^0_{[O]} - n_{[O]}(t)\right) \tag{12}$$

Figure 7 shows a graphical representation of Equation (12) for the case when the surface of the graphite penetrator is equal to 22.5 cm^2. As can be seen, the copper recovery process can be split up into two stages. In the first one, a rapid increase of $dn_{[O]}/dt$ is observed. This is probable due to the penetrator's surface activation. However, at the same time, the concentrations of the Cu_2O, PbO and Fe_2O_3 species in the slag decrease very fast. In the second stage, a monotonic slowdown of the reduction rate is observed. In the case of the computations, the second stage was limited to 4000 seconds, because, after this time, the $dn_{[O]}/dt$ values were very small. The logarithm of such small numbers goes to minus infinity, and so, it has an unjustifiably large influence on the parameters of the straight line. The parameters of this straight line are equal to $\ln(S \cdot k)$ and to the exponent n.

With the use of the data obtained in the second stage (**Figure 7**) as well as the least square method, the parameters k and n were calculated. **Table 3** contains these calculated parameters.

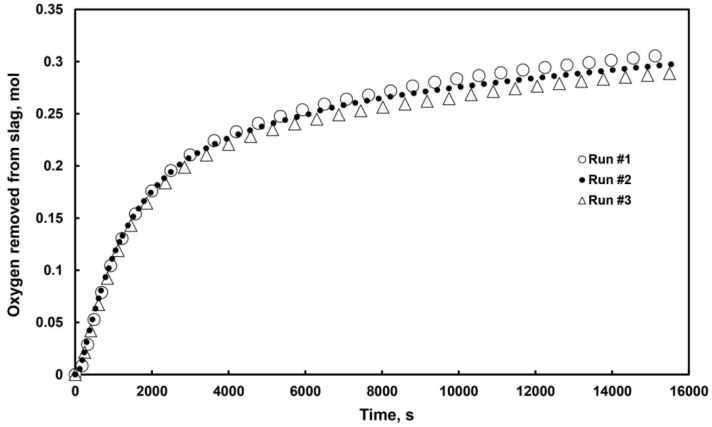

Figure 5. A relation between the number of the oxygen moles removed from the slag as a function of the reduction time at 1573 K. The surface of the used graphite penetrators was 22.5 cm^2. For the sake of graph clarity, only about 1/10 of the experimental points are shown.

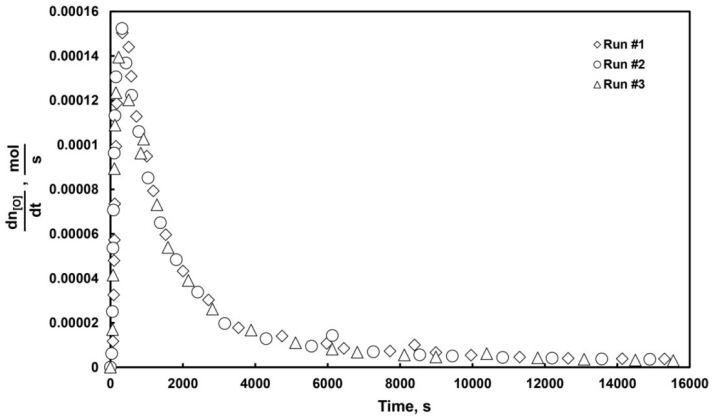

Figure 6. The rate of the oxygen removal $\left(dn_{[O]}/dt\right)$ from the reduced slag as a function of time. For the sake of graph clarity, only about 1/10 of the experimental points are shown.

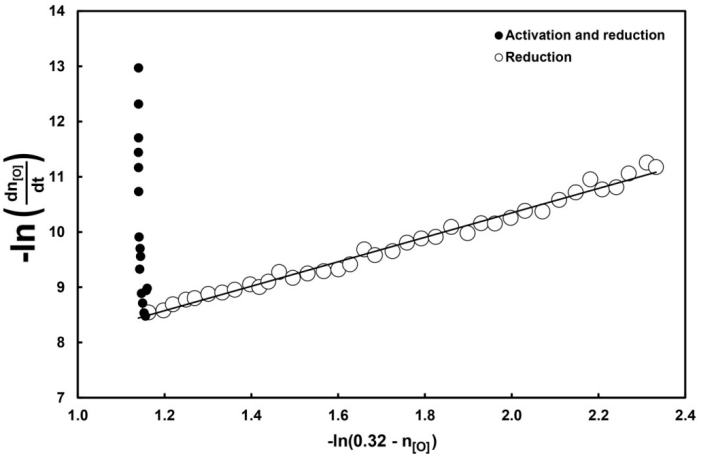

Figure 7. Graphical representation of the relation (12) for the case when the penetrator' surface is equal to 22.5 cm^2. For the sake of graph clarity, only about 1/10 of the experimental points are shown.

Table 3. The parameters of Equation (12) calculated with the points obtained from the experiments at 1573 K for various penetrator surfaces.

S, cm^2	$\ln\left(\frac{\mathrm{d}n_{[o]}}{\mathrm{d}t}\right) = \ln(S \cdot k) + n \cdot \ln\left(n^0_{[o]} - n_{[o]}(t)\right)$	k
16.1	$-6.2912 + 2.31 \cdot \ln\left(0.32 - n_{[o]}(t)\right)$	1.15×10^{-4}
16.1	$-6.5151 + 2.10 \cdot \ln\left(0.32 - n_{[o]}(t)\right)$	0.92×10^{-4}
16.1	$-5.9400 + 2.37 \cdot \ln\left(0.32 - n_{[o]}(t)\right)$	1.63×10^{-4}
22.5	$-6.0567 + 2.11 \cdot \ln\left(0.32 - n_{[o]}(t)\right)$	1.04×10^{-4}
22.5	$-5.9221 + 2.21 \cdot \ln\left(0.32 - n_{[o]}(t)\right)$	1.19×10^{-4}
22.5	$-5.9234 + 2.26 \cdot \ln\left(0.32 - n_{[o]}(t)\right)$	1.19×10^{-4}
29.8	$-4.8607 + 2.55 \cdot \ln\left(0.32 - n_{[o]}(t)\right)$	2.60×10^{-4}
29.8	$-4.5994 + 2.77 \cdot \ln\left(0.32 - n_{[o]}(t)\right)$	3.37×10^{-4}
29.8	$-4.7031 + 2.75 \cdot \ln\left(0.32 - n_{[o]}(t)\right)$	3.04×10^{-4}
37.9	$-4.6897 + 2.63 \cdot \ln\left(0.32 - n_{[o]}(t)\right)$	3.08×10^{-4}
37.9	$-4.3358 + 2.86 \cdot \ln\left(0.32 - n_{[o]}(t)\right)$	3.45×10^{-4}
37.9	$-4.3885 + 2.87 \cdot \ln\left(0.32 - n_{[o]}(t)\right)$	3.27×10^{-4}

The variation of k and n for different penetrator surfaces is illustrated in **Figure 8** and **Figure 9**.

After each experiment, the reduced slag was quenched and analyzed. The obtained results are enclosed in **Table 4** and **Table 5**. The reduced Cu-Pb-Fe alloys were also analyzed, and the results are given in **Table 6**.

The reduced Cu-Pb-Fe alloys were also analyzed, and the results are given in **Table 6**.

The Cu-Pb-Fe system exhibits a limited solubility in the liquid and the solid states, and the samples of these alloys were taken from different places with the purpose to secure their representativeness.

6. Conclusions

1) The influence of the reducer's surface on the rate of the slag de-coppering process is demonstrated in **Figure 10**. It is clear that, during this process, the copper, lead and iron are reduced simultaenously but at diffrent rates, forming the Cu-Pb-Fe alloy. The employed experimental technique is unable to determine the reduction rates of the particular metal oxides. **Figure 10** suggests that the effectiveness of the slag de-coppering process increases with the increase of the reducer's surface.

2) The reaction rate "constant" increases with the increase of the reducer's surface (see **Figure 8**) as well as the parameter n (see **Figure 9**). The increase of the reaction rate "constant" is, at least to some extent, compensated by the increase of the exponent n, as can be deduced from **Figure 11**.

3) The reduction process in the second stage was probably controlled by the convective mass transfer. This hypothesis can be justified by the magnitude of the exponent n and its change with the reducer's surface increase. When we used the penetrator with the biggest surface, the gap between the penetrator and the crucible wall was much smaller than that in the case when the smallest penetrator was employed. **Figure 12** shows the mutual position of the penetrators of limited sizes with the crucible during the experiments. When the penetrator with the biggest surface is employed, most of the generated gases pass through the smallest area of the cross

section between the penetrator and the crucible wall. In this case, the slag is more vigorously agitated. This situation prompts a transport of Cu_2O, PbO and Fe_2O_3 to the reduction surface. Consequently, we can infer that, in the industrial process, this phenomenon would not take place, because the size of the electric furnace is much bigger than that of a crucible used in a laboratory experiment. Even in the case of the laboratory experiment, the reaction rate referred to the surface unit can be taken as a constant (see **Figure 11**) if we assume that every measurement is determined with a certain error.

4) The overall rate of the oxygen removal from the slag increases with the reducer's surface increase, as can be seen in **Figure 13**.

5) The reduction process in the second stage is very likely to be controlled by the convective mass transfer. When the penetrator with the biggest surface is employed, more gases (CO + CO_2) are generated in a time unit, which have to pass through the smallest area of the cross section between the penetrator and the crucible wall. In consequence, the superficial gas velocity increases, as can be seen in **Figure 14** and this induces a stronger convective flow of the reduced slag.

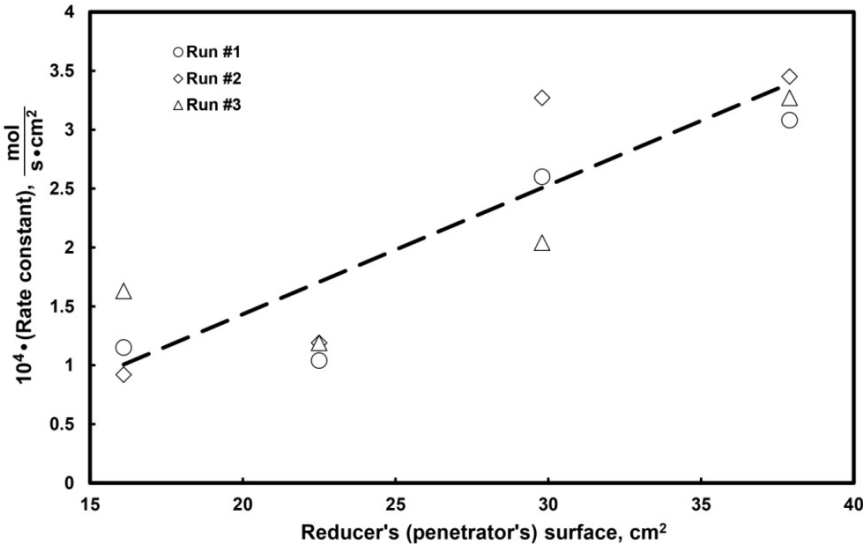

Figure 8. Dependence of the reaction rate constant (*k*) on the surface of the reducer (penetrator).

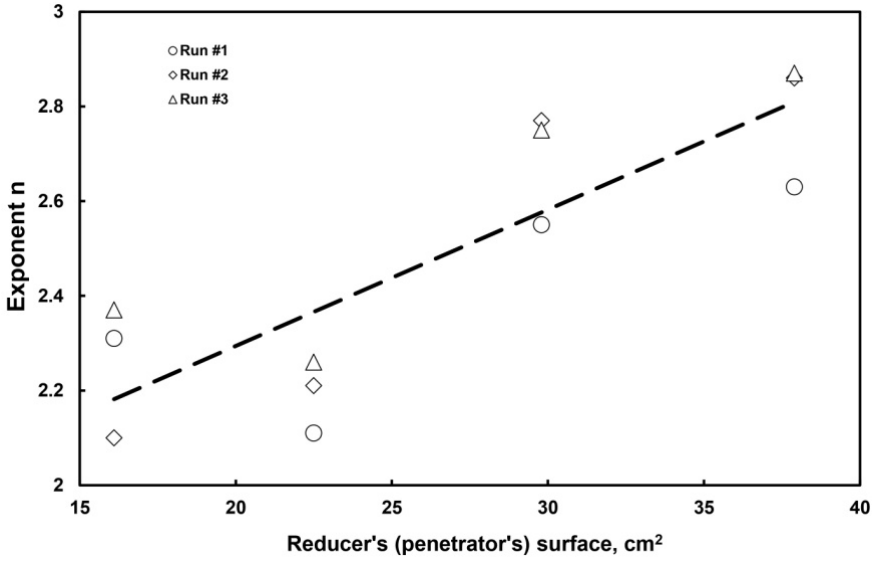

Figure 9. Dependence of the parameter *n* on the surface of the reducer (penetrator).

Table 4. Results of the chemical analyses of the slags after the reduction process with the use of different graphite penetrators.

Component, wt. -%	S = 16.1 cm^2			S = 22.5 cm^2		
	Run #1	Run #2	Run #3	Run #1	Run #2	Run #3
Na_2O	0.74	0.74	0.73	0.71	0.74	0.73
K_2O	3.29	3.29	3.92	3.33	3.30	3.50
CaO	20.63	20.63	22.30	21.05	20.80	21.48
MgO	7.33	7.33	8.28	7.41	7.54	7.59
Al_2O_3	12.25	12.25	14.52	12.80	12.80	13.35
SiO_2	35.6	38.3	30.38	38.2	38.9	36.50
Fe	10.82	10.82	12.52	10.67	10.78	11.29
Zn	0.87	0.87	0.97	0.74	0.50	0.51
Pb	0.32	0.32	0.20	0.237	0.210	0.228
Cu	0.23	0.23	0.19	0.22	0.29	0.22

Table 5. Results of the chemical analyses of the slags after the reduction process with the use of different graphite penetrators.

Component, wt. -%	S = 29.8 cm^2			S = 37.9 cm^2		
	Run #1	Run #2	Run #3	Run #1	Run #2	Run #3
Na_2O	0.73	0.71	0.85	0.75	0.89	0.85
K_2O	3.40	4.05	3.85	3.45	3.92	3.69
CaO	21.66	23.11	22.55	21.89	23.15	21.79
MgO	7.86	8.60	8.30	7.73	8.45	7.97
Al_2O_3	12.91	14.94	15.97	12.99	17.22	19.43
SiO_2	36.7	29.89	30.00	36.9	28.62	28.21
Fe	11.03	12.49	12.25	10.63	12.33	11.64
Zn	0.50	0.50	0.50	0.47	0.45	0.49
Pb	0.10	0.06	0.06	0.08	0.07	0.07
Cu	0.13	0.13	0.11	0.10	0.12	0.13

Table 6. Results of the chemical analyses of the Cu-Pb-Fe alloys obtained during the slag reduction with the use of different graphite penetrators.

Component, wt. -%	S = 16.1 cm^2			S = 22.5 cm^2		
	Run #1	Run #2	Run #3	Run #1	Run #2	Run #3
Cu	88.73	85.65	85.81	85.92	84.41	85.74
Pb	11.14	14.62	13.14	13.53	15.38	14.16
Fe	0.16	0.27	0.87	0.56	0.92	0.62
	S = 29.8 cm^2			S = 37.9 cm^2		
Cu	84.86	84.57	84.52	84.52	85.03	85.82
Pb	14.14	14.57	13.80	13.77	13.90	12.25
Fe	1.5	1.43	1.70	1.56	1.80	1.68

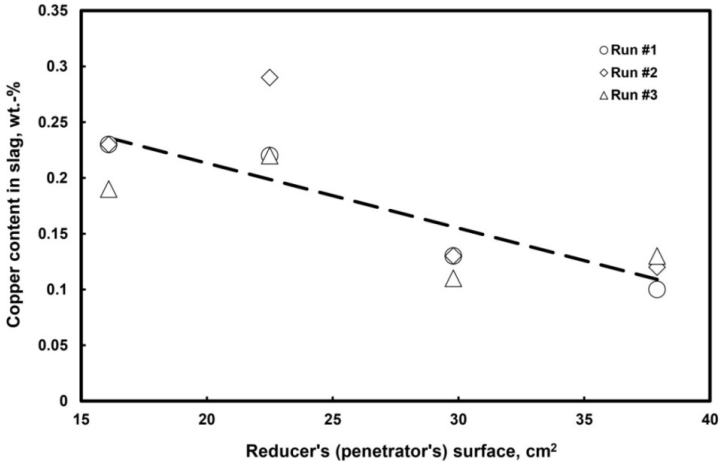

Figure 10. Relation between the final copper content in the slag and the reducer's surface.

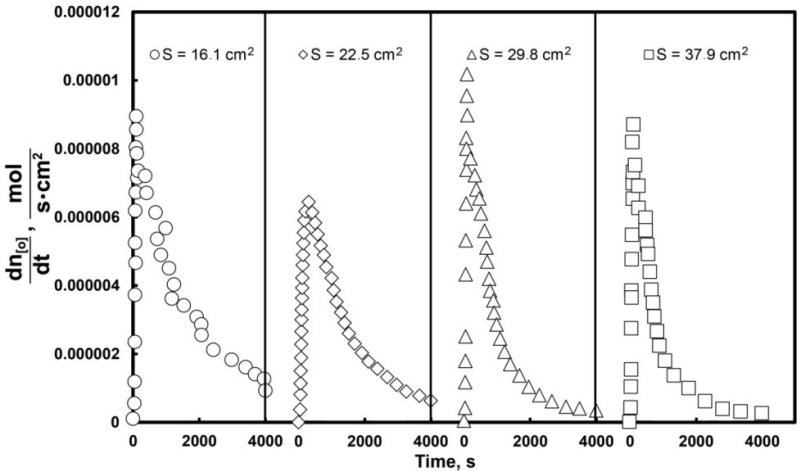

Figure 11. Rate of the oxygen removal from the slag as a function of time for reducers (penetrators) of different surfaces and referred to the surface unit. For the sake of graph clarity, only about 1/10 of the experimental points are shown.

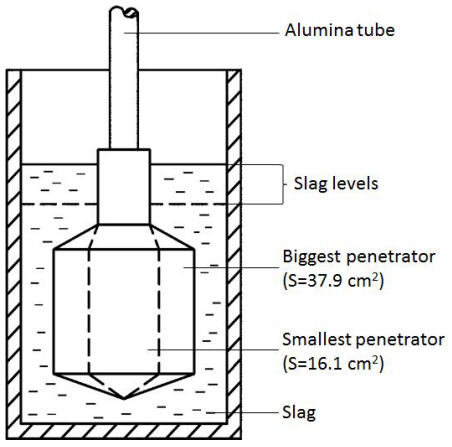

Figure 12. The mutual position of the penetrators of limited sizes and the crucible wall during the experiments.

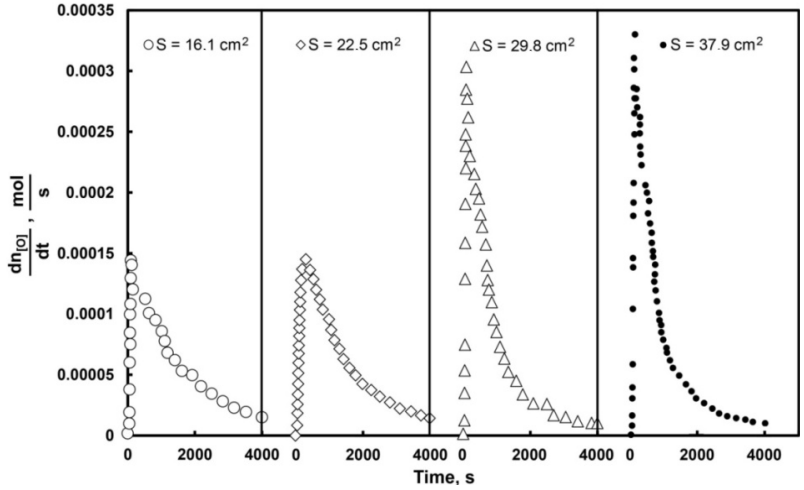

Figure 13. The overall rate of the oxygen removal from the slag for different penetrator surfaces. For the sake of graph clarity, only about 1/10 of the experimental points are shown.

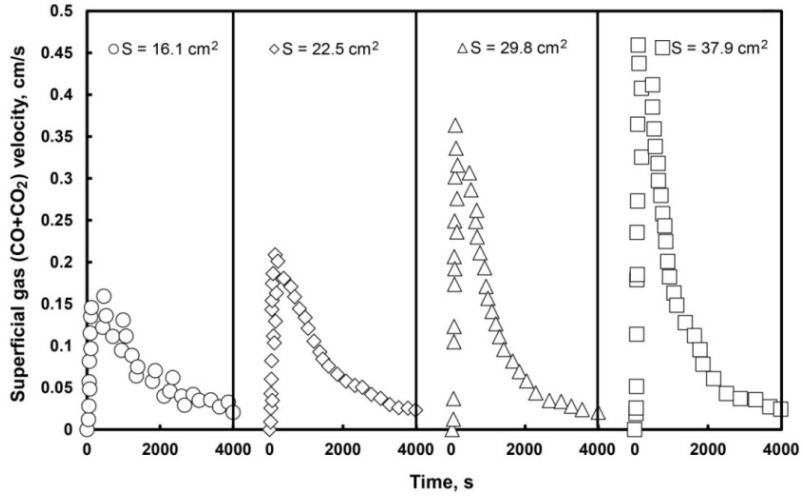

Figure 14. Relation between the superficial gas velocity and the time for various sizes of the graphite penetrators.

Acknowledgements

We would like to thank the Polish National Center Research and Development (NCBiR) for the financial support—Grant No. 07-0022-10.

References

[1] Kondakov, V.V., Ryzhonkov, D.I. and Golenko, D.M. (1960) Issledovanie kinetiki vosstanovleniâ zakisi železa tverdym uglerodom pri temperaturah vyše 1400. *Izvestiya Vysshikh Uchebnykh Zavedenii*, *Chernaya Metallurgiya*, **4**, 23-28.

[2] Krainer, H., Beer, H.P. and Brandl, H. (1966) Untersuchung über die Reactionen flüssiger hocheisen(II)-oxidhaltiger Schlacken mit festem Kohlenstoff. *Technische Mitteilungen Krupp Forschungsberichte*, **24**, 139-146.

[3] Fay, F. (1970) Rates and Mechanism of FeO Reduction from Slags. *Metallurgical Transactions*, **1**, 2537-2541.

[4] Shalimov, M.P., Boronenkov, V.N. and Lyamkin, S.A. (1980) Mehanizm i kinetika vzaimodeistviâ rasplavov FeO-SiO_2, suglerodom. *Metally*, **6**, 32-36.

[5] Sato, A., Aragane, G., Kamihira, K. and Yoshimatsu, S. (1987) Reducing Rates of Molten Iron Oxide by Solid Carbon

or Carbon in Molten Iron. *Transactions of ISIJ*, **27**, 789-796.

[6] Min, D.-J. and Fruehan, R.J. (1992) Rate of Reduction of FeO in Slag by Fe-C Drops. *Metallurgical and Materials Transactions B*, **23B**, 29-37.

[7] Paramguru, R.K., Galgali, R.K. and Ray, H.S. (1977) Influence of Slag and Foam Characteristics on Reduction of FeO-Containing Slags by Solid Carbon. *Metallurgical and Materials Transactions B*, **28B**, 805-810.

[8] Warczok, A. and Utigard, T.A. (1998) Fayalite Slag Reduction by Solid Graphite. *Canadian Metallurgy Quarterly*, **37**, 27-39. http://dx.doi.org/10.1179/cmq.1998.37.1.27

[9] Min, D.J., Han, J.W. and Chung, W.S. (1999) A Study of the Reduction Rate of FeO in Slag by Solid Carbon. *Metallurgical and Materials Transactions B*, **30B**, 215-221.

[10] El-Rassi, K.P. and Utigard, T.U. (2000) Rate of Slag Reduction in a Laboratory Electric Furnace—Alternating vs Direct Current. *Metallurgical and Materials Transactions B*, **31B**, 1187-1194.

[11] Mróz, J. (2001) Evaluation of the Reduction of Iron Oxide from Liquid Slags Using a Graphite Rotating Disk. *Metallurgical and Materials Transactions B*, **32**, 821-830. http://dx.doi.org/10.1007/s11663-001-0069-8

[12] Grieveson, P. and Turkdogan, E.T. (1964) Kinetics of Oxidation and Reduction of Molten Iron Oxide. *Transactions of the Metallurgical Society of AIME*, **230**, 1609-1614.

[13] Sasaki, Y., Hara, S., Gaskell, D.R. and Belton, G.R. (1984) Isotope Exchange Studies of the Rate of Dissociation of CO_2 on Liquid Iron Oxides and CaO-Saturated Calcium Ferrites. *Metallurgical Transactions B*, **15**, 563-571. http://dx.doi.org/10.1007/BF02657388

[14] Utigard, T., Sunchez, G., Manriquez, J., Lurashi, A., Diaz, C., Cordero, D. and Almendras, E. (1997) Reduction Kinetics of Liquid Iron Oxide-Containind Slags by Carbon Monoxide. *Metallurgical and Materials Transactions B*, **28**, 821-826. http://dx.doi.org/10.1007/s11663-997-0009-3

[15] Sun, S. and Belton, G.R. (1998) The Effect of Surfactants on the Interfacial Rates of Reaction of CO_2 and CO with Liquid Iron Oxide. *Metallurgical and Materials Transactions B*, **29**, 137-145. http://dx.doi.org/10.1007/s11663-998-0016-z

[16] Nagasaka, T., Hino, M. and Ban-Ya, S. (2000) Interfacial Kinetics of Hydrogen with Liquid Slag Containing Iron Oxide. *Metallurgical and Materials Transactions B*, **31**, 945-955. http://dx.doi.org/10.1007/s11663-000-0071-6

[17] Ratchev, I.P. (2002) Rate of Interfacial Reaction between Molten $CaO\text{-}SiO_2\text{-}Al_2O_3\text{-}Fe_xO$ and $CO\text{-}CO_2$. *Metallurgical and Materials Transactions B*, **33**, 651-660.

[18] Barati, M., Chen, E. and Coley, K. (2004) A Comparison of the Kinetics of the $CO\text{-}CO_2$ Reaction with Steelmaking and Copper Making Slags. *VII International Conference on Molten Slags Fluxes and Salts*, The South African Institute of Mining and Metallurgy, 393-398.

[19] Barati, M. and Coley, K.S. (2005) Kinetics of $CO\text{-}CO_2$ Reactions with $CaO\text{-}SiO_2\text{-}FeO_x$ Melts. *Metallurgical and Materials Transactions B*, **36**, 169-178. http://dx.doi.org/10.1007/s11663-005-0017-0

[20] Kucharski, M., Sak, T., Madej, P., Wędrychowicz, M. and Mróz, W. (2014) A Study on the Copper Recovery from the Slag of the Outokumpu Direct-to-Copper Process. *Metallurgical and Materials Transactions B*, **45**, 590-602. http://dx.doi.org/10.1007/s11663-013-9961-2

[21] Rogóż, K. and Kucharski, M. (2010) The Rate of Metal Oxides Reduction from the Slag of the Direct-to-Blister Flash Smelting Process. *Archives of Metallurgy and Materials*, **55**, 317-323.